IEEE Photonics Journal
An IEEE Photonics Society Publication

Open Access

Single-Notch Microwave Photonic Filter Using a Nonsliced ASE Source and a Laser Diode

Volume 8, Number 1, February 2016

Wei Li
Cheng Wu Yang
Ling Wang
Jian Guo Liu
Ning Hua Zhu, Member, IEEE

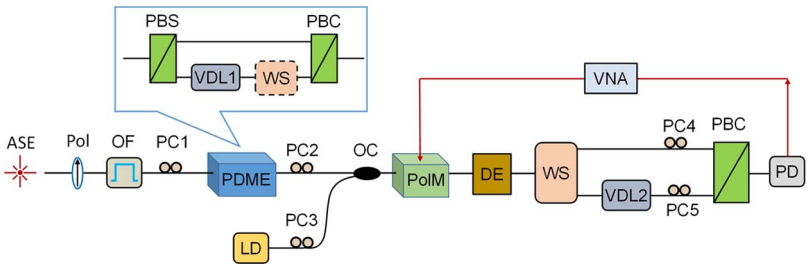

DOI: 10.1109/JPHOT.2015.2510637
1943-0655

Single-Notch Microwave Photonic Filter Using a Nonsliced ASE Source and a Laser Diode

Wei Li, Cheng Wu Yang, Ling Wang, Jian Guo Liu, and Ning Hua Zhu, *Member, IEEE*

State Key Laboratory on Integrated Optoelectronics, Institute of Semiconductors, Chinese Academy of Sciences, Beijing 100083, China

DOI: 10.1109/JPHOT.2015.2510637

Manuscript received November 23, 2015; revised December 12, 2015; accepted December 16, 2015. Date of publication December 23, 2015; date of current version January 5, 2016. This work was supported in part by the National Natural Science Foundation of China under Grant 61377069, Grant 61335005, and Grant 61431003; by the National High Technology Research and Development Program (863 Program) under Grant 2015AA017002; by the National Basic Research Program of China (973 Program) under Grant 2012CB315703; and by the Beijing Nova Program under Grant xxjh2015B076. Corresponding author: N. H. Zhu (e-mail: nhzhu@semi.ac.cn).

Abstract: We present a continuously tunable single-notch microwave photonic filter (MPF) using polarization processing of a nonsliced amplified spontaneous emission (ASE) source and a laser diode (LD). The ASE source is used to generate a single-passband MPF, whereas the LD is used to realize a broadband microwave photonic phase shifter (MPS). By destructive interfering between the single-passband MPF and the MPS, a widely tunable single-notch MPF is achieved. The proposed method has been theoretically analyzed and experimentally verified.

Index Terms: Microwave photonic filter (MPF), polarization modulation.

1. Introduction

Microwave photonic filter (MPF) has been a hot topic in microwave and millimeter-wave signal processing applications [1], [2]. They have many advantages over the conventional electronic-based approach, such as high bandwidth, wide tunability, and electron-magnetic interference immunity. Microwave photonic notch filters are preferred in many applications. They are widely used to remove the unwanted clutter and noise from the desired signals in radars and fiber-based antenna arrays.

Up to now, many microwave photonic notch filters have been reported [3]–[6]. Microwave photonic notch filters can be realized using delay lines, which are the so-called finite impulse response (FIR) filters. A multi-tap filter with complex coefficient has a tunable notch response [5]. The shape of the filter keeps unchanged during frequency tuning. However, the selectivity of the filter is limited by the number of the taps, which is not reconfigurable for a given structure. The infinite impulse response (IIR) MPFs benefit from the high-resolution narrow notch response, but the small free spectral range (FSR) limits its applications in wideband signal processing [7], [8].

Microwave photonic notch filters have also been achieved using sliced broadband optical source (BOS), fiber Bragg grating (FBG), and stimulated Brillouin scattering (SBS) [9]–[11].

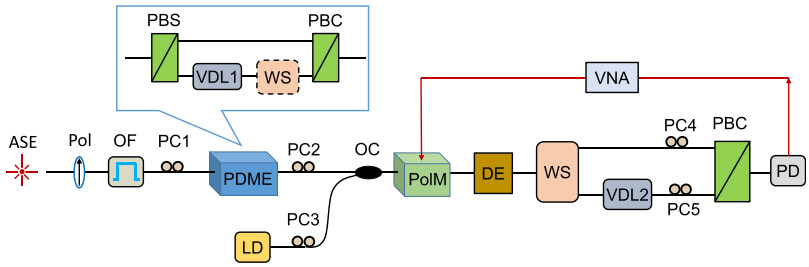

Fig. 1. Schematic diagram of the proposed single-notch MPF. ASE: amplified spontaneous emission; Pol: polarizer; OF: optical filter; PC: polarization controller; PDME: polarization division multiplexing emulator; PBS: polarization beam splitter; PBC: polarization beam combiner; VDL: variable delay line; WS: wave shaper; PolM: polarization modulator; DE: dispersive element; VNA: vector network analyzer; PD: photodetector.

However, the sliced BOS-based method suffers from double-notch response [9]. The single-notch MPF using FBG suffers from the frequency drift between the tunable laser diode and the FBG resonance. Microwave photonic single-notch filters based on SBS is capable of implementing very narrow notch. However, long optical fiber is usually required to generate SBS, which makes the system complicated and bulky. Recently, on-chip SBS has been used to achieve single-notch MPF, which avoids the use of bulky optical fibers [12]. However, ultrafine control of the three biases of the dual-parallel Mach–Zehnder modulator (DPMZM) is required. Recently, microwave photonic notch filter with ultra-fast tunability has been reported [13]. The filter can reach a recorded tuning speed of less than 100 ps. In [14], we reported a single-passband MPF using polarization processing of ASE source.

In this paper, we propose and demonstrate a single-notch MPF based on polarization processing of a non-sliced ASE source and a LD. The non-sliced ASE source generates a single-passband MPF, while the LD is used to achieve a broadband MPS. The destructive interference between the single-passband MPF and the broadband MPS generates a single-notch MPF. The center frequency of the notch MPF is widely tunable by adjusting an optical delay line. The proposed approach is theoretically analyzed and experimentally verified.

2. Principle and Simulation

The schematic structure of the proposed single-notch MPF is illustrated in Fig. 1. In our proposed MPF, an ASE source and a LD are used as the optical sources. The non-sliced ASE source is used to achieve a single-passband MPF. The LD is used to realize a broadband MPS. By properly adjusting the phase shift, a single-notch MPF can be generated. In the proposed structure, the ASE source is polarized by a polarizer (Pol) and filtered to be rectangular shape by an optical filter (OF). The electrical field can be expressed as

$$E_{\mathrm{ASE}}(t) = \frac{1}{2\pi}\int_{0}^{\infty} E(\Omega)e^{j\Omega t}\,d\Omega \tag{1}$$

where Ω is the angular frequency of the ASE source. The center frequency of the ASE source is denoted as Ω_0. The stochastic property of $E(\Omega)$ is given by

$$\langle E(\Omega)E^{*}(\Omega')\rangle = 2\pi N(\Omega)\delta(\Omega-\Omega') \tag{2}$$

where $N(\Omega)$ is the power spectral density. The ASE signal is sent to a commercial available polarization division multiplexing emulator (PDME) which consists of a polarization beam splitter (PBS), an optical variable delay line (VDL1), and a polarization beam combiner (PBC). The function of a wave shaper (WS) cascaded behind the VDL1 will be discussed in the next section. Here, we ignore the WS in the following discussion. A polarization controller (PC1) is

used to balance the power splitting ratio between the two orthogonal polarization states of the PDME. The electrical field at the output of the PDME is given by

$$E_{\mathrm{PDME}}(t) = \begin{bmatrix} E_{\parallel}(t) \\ E_{\perp}(t) \end{bmatrix} = \frac{1}{\sqrt{2}} \begin{bmatrix} E_{\mathrm{ASE}}(t) \\ E_{\mathrm{ASE}}(t-\Delta\tau) \end{bmatrix} \tag{3}$$

where $\Delta\tau$ is the delay time of the VDL1. A laser diode (LD) emitting at angular frequency of Ω_1 is coupled with the ASE source by an optical coupler (OC). The combined optical signals are sent to a polarization modulator (PolM). The PolM is a special phase modulator with opposite phase modulation index at two orthogonal principal axes. The state of polarizations (SOPs) of the ASE source and the LD are controlled by PC2 and PC3, respectively. The electrical fields of ASE source, $E_{\perp}(t)$ and $E_{\parallel}(t)$, are aligned at an angle of 45° and 135° with respect to one principal axis of the PolM, respectively. The SOP of the LD is aligned at an angle of 45° to one principal axis of the PolM. After polarization modulation, two first-order sidebands are generated at both sides of an optical carrier under small-signal modulation condition. The SOP of the optical carrier is orthogonal to that of the first-order optical sidebands. The frequency domain optical signal is written as

$$E^{\mathrm{ASE}}_{\mathrm{PolM}}(\Omega) = \begin{bmatrix} E_{\parallel}(\Omega) \\ E_{\perp}(\Omega) \end{bmatrix} = \frac{1}{\sqrt{2}} \begin{bmatrix} E(\Omega) + cE(\Omega+\omega_m)e^{-j(\Omega+\omega_m)\Delta\tau} + cE(\Omega-\omega_m)e^{-j(\Omega-\omega_m)\Delta\tau} \\ E(\Omega)e^{-j\Omega\Delta\tau} + cE(\Omega+\omega_m) + cE(\Omega-\omega_m) \end{bmatrix} \tag{4}$$

$$E^{\mathrm{LD}}_{\mathrm{PolM}}(\Omega) = \begin{bmatrix} E_{\parallel}(t) \\ E_{\perp}(t) \end{bmatrix} = \frac{E_1}{\sqrt{2}} \begin{bmatrix} c\delta(\Omega-\Omega_1-\omega_m) + c\delta(\Omega-\Omega_1+\omega_m) \\ \delta(\Omega-\Omega_1) \end{bmatrix} \tag{5}$$

where ω_m is the angular frequency of the microwave signal applied to the PolM, c is the modulation index of the PolM, and Ω_1 is the angular carrier frequency of the LD. E_1 is the amplitude of the LD. A dispersive element (DE) is used as an optical phase filter, whose phase dependence can be developed by a Taylor expansion centered at Ω_0 [15]

$$\Phi(\Omega) = \Phi(\Omega_0) + \tau_0(\Omega_0)(\Omega-\Omega_0) + \frac{1}{2}\beta(\Omega-\Omega_0)^2 \tag{6}$$

where $\tau_0(\Omega_0)$ is the group delay time at Ω_0, and β is the total dispersion of the DE. The electrical field after DE is given by

$$E_{\mathrm{DE}}(\Omega) = \left[E^{\mathrm{ASE}}_{\mathrm{PolM}}(\Omega) + E^{\mathrm{LD}}_{\mathrm{PolM}}(\Omega)\right] e^{j\Phi(\Omega)}. \tag{7}$$

A WS is attached after the DE to separate the ASE and LD signals. It is worth noting that one of the first-order sidebands of the LD is removed by the WS in order to overcome the dispersion induced power fading. A PBC is used to couple the ASE and LD signals to a photodetector (PD). A PC4 is used to adjust the SOP of the polarization-modulated ASE signal to remove the $E_{\parallel}(\Omega)$ component using the PBC. On the other hand, a PC5 is used to adjust the SOP of the polarization modulated LD signal and to add an additional phase difference between the optical carrier and the first order sideband. The optical carrier of LD is aligned at 45° to the PBC. A delay time T_0 is introduced by a VDL2 to compensate for the group delay difference between the ASE and LD. The electrical field after the PBC is written as

$$E_{\mathrm{PBC}}(\Omega) = \begin{bmatrix} E_{\mathrm{ASE}}(\Omega) \\ E_{\mathrm{LD}}(\Omega) \end{bmatrix} \propto e^{j\Phi(\Omega)} \begin{bmatrix} E(\Omega)e^{-j\Omega\Delta\tau} + cE(\Omega+\omega_m) + cE(\Omega-\omega_m) \\ E_1\delta(\Omega-\Omega_2)e^{-j(\Omega T_0+\varphi)} + cE_1\delta(\Omega-\Omega_2-\omega_m) \end{bmatrix} \tag{8}$$

where φ is the phase shift between the optical carrier of LD and the first-order sideband, which is introduced by the PC5. The photocurrent can be expressed as

$$I(\omega) = \frac{1}{2\pi}\left\langle \int_0^{\infty} E_{\mathrm{ASE}}(\Omega)E^{*}_{\mathrm{ASE}}(\Omega-\omega)d\Omega \right\rangle + \frac{1}{2\pi}\left\langle \int_0^{\infty} E_{\mathrm{LD}}(\Omega)E^{*}_{\mathrm{LD}}(\Omega-\omega)d\Omega \right\rangle. \tag{9}$$

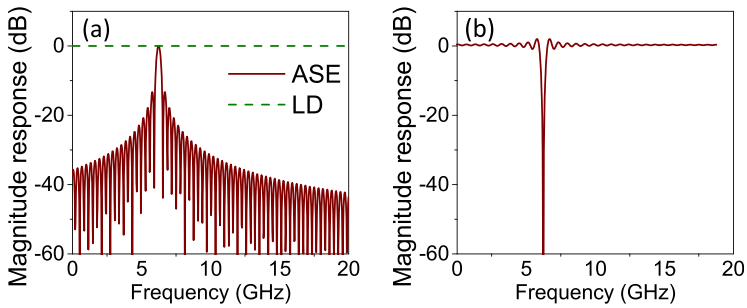

Fig. 2. Simulated transfer functions of (a) the single-passband MPF generated by non-sliced ASE source and the LD and (b) the single-notch MPF.

If we only consider the frequency components at $\omega > 0$, the transfer function of the MPF is written as

$$H(\omega) \propto I_{\mathrm{ASE}}(\omega) + I_{\mathrm{LD}}(\omega) = e^{-j\left(\omega\tau_0 + \frac{1}{2}\beta\omega^2 - \omega\beta\Omega_0\right)} \cdot \left[e^{j\beta\omega\Omega_0} \cdot H_{\mathrm{ASE}}\left(\Omega - \frac{\Delta\tau}{\beta}\right) + E_1^2 e^{-j[\omega\beta(\Omega_1 - \Omega_0) + \omega T_0 + \varphi]} \right]. \tag{10}$$

where $H_{\mathrm{ASE}}(\Omega)$ is the baseband response given by

$$H_{\mathrm{ASE}}(\Omega) = \frac{1}{2\pi} \int_0^\infty N(\Omega)\ \mathrm{e}^{-j\omega\beta\Omega}\, d\Omega. \tag{11}$$

As can be seen from (10), the finally generated MPF has two parts: One is a single passband MPF, and the other is a broadband MPS [16]. Our desired single-notch MPF can be realized by interfering between the single-passband MPF and the broadband MPS. The amplitude and phase requirement can be written as

$$\frac{1}{2\pi} \int_0^\infty N(\Omega)\, d\Omega = E_1^2 \tag{12a}$$

$$T_0 = 2\beta\Omega_0 - \beta\Omega_1, \quad \varphi = \pi. \tag{12b}$$

As indicated by (12), the delay time T_0 introduced by VDL2 is determined by the wavelength of the two optical sources, as well as β of the dispersive fiber. If the wavelength of the two optical sources is changed, the delay time should be tuned accordingly. Fig. 2(a) plots the simulated transfer functions generated by ASE and LD. The parameters used in our simulations are extracted from our experiments which will be clear later. The ASE source results in a single passband MPF, while the LD generates a broadband MPS with fixed amplitude. Under amplitude and phase matching condition, a single-notch MPF is realized as shown in Fig. 2(b). The center frequency of the notch MPF is continuously tunable by adjusting the VDL1, $\Delta\tau$.

3. Experiments and Results

An experiment based on the configuration shown in Fig. 1 was carried out. The filtered ASE source has a center frequency of 1550.20 nm and a bandwidth of 8 nm. After passing through a PDME, the ASE signal was coupled with a LD at 1555.72 nm. They were modulated by a PolM with a bandwidth of 40 GHz. The optical signal at the output of the PolM is shown in Fig. 3(a). In this case, the PolM was driven by a microwave signal at 10 GHz. The DE used in our experiment has a total dispersion of 5.08×10^{-22} s^2. A WS (Finisar 4000S) was used to separate the ASE and LD signals. The separated ASE signal is shown in Fig. 3(b), where the undesired LD signal was 23 dB lower than the ASE signal. On the other channel of the WS, the ASE signal was

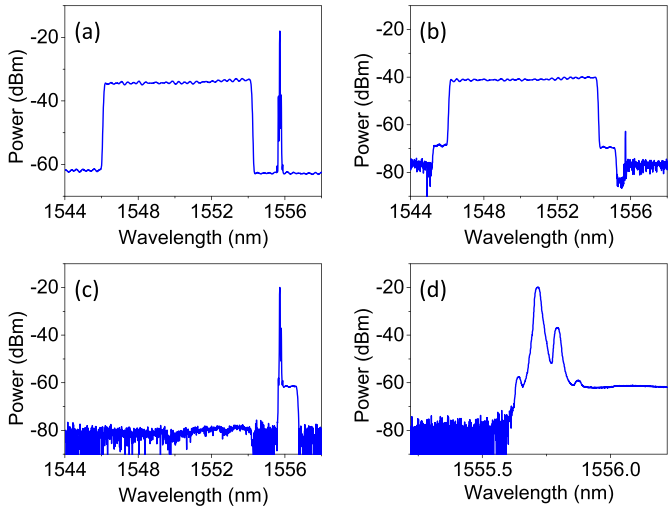

Fig. 3. Measured optical spectra of (a) polarization modulated ASE and LD signals, (b) selected ASE signal, (c) selected LD signal, and (d) zoom-in view of the LD signal.

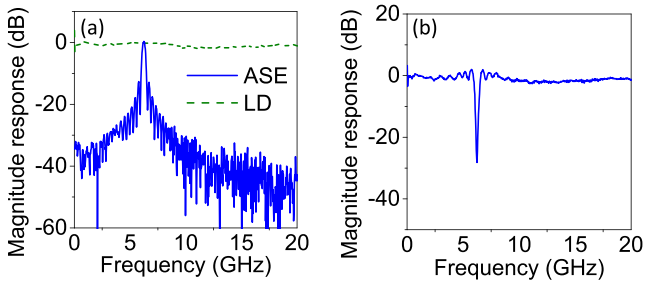

Fig. 4. Measured transfer functions of (a) single-passband MPF generated by non-sliced ASE source and the LD and (b) single-notch MPF.

suppressed as shown in Fig. 3(c). In addition, single-sideband (SSB) modulation was also realized using the WS. The zoom-in view of Fig. 3(c) is illustrated in Fig. 3(d). The SSB suppression ratio was measured to be 17 dB. The PCs and VDL2 were adjusted as described in Section 2. A PD with a bandwidth of ~20 GHz was used to detect the microwave signals. A vector network analyzer (VNA) with a bandwidth of 40 GHz was used to measure the transfer response of the MPF.

The transfer responses of the MPFs generated by ASE source and LD are shown in Fig. 4(a). The ASE source generates a single-passband MPF which is centered at 6.24 GHz, corresponding to a delay time of $\Delta\tau = 20$ ps. Meanwhile, a broadband MPS was generated by the LD on the other orthogonal polarization state. The phase of the MPS is continuously tunable from 0° to 360°. Detail analysis of the MPS can be found in our previous work [17]. The single-passband MPF and the broadband MPS interfered with each other in the PD, which results in a single-notch MPS as shown in Fig. 4(b). The notch suppression ratio is around 30 dB. In principle, the suppression ratio of the notch should be unlimited; see Fig. 2(b). However, a limited suppression ratio of ~30 dB was achieved in our experiment due to the unmatched amplitude and phase conditions of the single-passband MPF and the MPS.

The 3-dB bandwidth of the single-notch MPF is measured to be ~500 MHz. The center frequency of the notch MPF is continuously tunable by adjusting delay time $\Delta\tau$. Fig. 5 shows the frequency tunability of the notch MPF. The center frequency of the notch MPF is tuned from 3 to 18 GHz. The working bandwidth of the MPS is limited by the WS because the WS has a limited roll-off edge, which means that the SSB modulation is imperfect in the low frequency

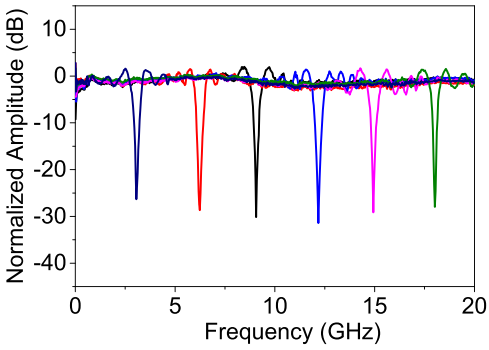

Fig. 5. Measured transfer function of the single-notch MPF by tuning the optical delay line.

range. Therefore, the working bandwidth of the generated single-notch MPF is also limited by the WS. As the tunability of the center frequency is realized by adjusting the delay line, it cannot realize fast tunability unless fast tunable optical true-time delay line is available.

In our scheme, many polarization sensitive elements are involved. The stability of the system thus suffers from the environmental fluctuation and temperature change. To ensure a stable operation of the system, polarization maintaining fibers should be used to connect these components. Moreover, an integrated MPF is more promising to overcome the limitations since most of the devices used in this scheme can be integrated.

As can be seen from the simulated and experimental results shown in Figs. 2(b), 4(b), and 5, the notch MPF has some ripples at the passband. This can be attributed to the sinc-function response of the bandpass MPF which is the Fourier transform of the ASE source. To flat the passband of the notch MPF, the other WS is added in the PDME as show in Fig. 1. The WS is a programmable optical filter with arbitrary amplitude and phase responses. The transfer function of the WS is denoted as

$$H_{\mathrm{WS}}(\Omega) = M_{\mathrm{WS}}(\Omega)\mathrm{e}^{j\Phi_{\mathrm{WS}}(\Omega)}. \tag{13}$$

In this case, the transfer response of the notch MPF can be rewritten as

$$H(\omega) = e^{-j\left(\omega\tau_0+\frac{1}{2}\beta\omega^2-\omega\beta\Omega_0\right)} \cdot \left[e^{j\beta\omega\Omega_0} \cdot H_M\left(\omega-\frac{\Delta\tau}{\beta}\right) + E_1^2 e^{-j[\omega\beta(\Omega_1-\Omega_0)+\omega T_0+\varphi]}\right] \tag{14}$$

where $H_M(\omega)$ is the baseband response given by

$$H_M(\omega) = \frac{1}{2\pi}\int_0^{\infty} H_{\mathrm{WS}}^*(\Omega)N(\Omega)e^{-j\omega\beta\Omega}\,d\Omega. \tag{15}$$

The single-notch MPF is related to the Fourier transform of the transfer function of the WS. Therefore, by programming the WS, arbitrary amplitude and phase of the notch MPF can be realized. The proposed notch MPF is highly reconfigurable and widely tunable.

4. Conclusion

We have proposed and demonstrated a single-notch MPF. The notch MPF was achieved by interfering between a single passband MPF and a broadband MPS. By polarization processing of a non-sliced ASE source, a widely tunable single-passband MPF was generated. On the other hand, a broadband MPS was generated by a LD. By adjusting the phase shift of the MPS, a single-notch MPF was generated. The proposed approach has been theoretically analyzed and experimentally verified. The center frequency of the notch MPF was widely tunable by adjusting the optical delay line. In addition, the notch MPF is highly reconfigurable by inserting the other WS in the PDME.

References

[1] R. A. Minasian, "Photonic signal processing of microwave signals," *IEEE Trans. Microw. Theory Techn.*, vol. 54, no. 2, pp. 832–846, Feb. 2006.

[2] J. Capmany, B. Ortega, and D. Pastor, "A tutorial on microwave photonic filters," *J. Lightw. Technol.*, vol. 24, no. 1, pp. 201–229, Jan. 2006.

[3] J. Wang and J. Yao, "A tunable photonic microwave notch filter based on all-optical mixing," *IEEE Photon. Technol. Lett.*, vol. 18, no. 2, pp. 382–384, Jan. 2006.

[4] W. Li, N. H. Zhu, and L. X. Wang, "Continuously tunable microwave photonic notch filter with a complex coefficient," *IEEE Photon. J.*, vol. 3, no. 3, pp. 462–467, Jun. 2011.

[5] Y. M. Zhang and S. L. Pan, "Tunable multitap microwave photonic filter with all complex coefficients," *Opt. Lett.*, vol. 38, no. 5, pp. 802–804, Mar. 2013.

[6] C. Zhang *et al.*, "A tunable microwave photonic filter with a complex coefficient based on polarization modulation," *IEEE Photon. J.*, vol. 5, no. 5, Oct. 2013, Art. ID 5501606.

[7] R. A. Minasian, K. E. Alameh, and E. H. W. Chan, "Photonics-based interference mitigation filters," *IEEE Trans. Microw. Theory Techn.*, vol. 49, no. 10, pp. 1894–1899, Oct. 2001.

[8] E. Xu, X. Zhang, L. Zhou, Y. Zhang, and D. Huang, "A simple microwave photonic notch filter based on a semiconductor optical amplifier," *J. Opt. A, Pure Appl. Opt.*, vol. 11, no. 8, May 2009, Art. ID 085405.

[9] Y. Yu, S. Li, X. Zheng, H. Zhang, and B. Zhou, "Tunable microwave photonic notch filter based on sliced broadband optical source," *Opt. Exp.*, vol. 23, no. 19, pp. 24 308–24 316, Sep. 2015.

[10] E. Xu and J. Yao, "Frequency- and notch-depth-tunable single-notch microwave photonic filter," *IEEE Photon. Technol. Lett.*, vol. 27, no. 19. pp. 2063–2066, Oct. 2015.

[11] W. Zhang and R. A. Minasian, "Ultrawide tunable microwave photonic notch filter based on stimulated Brillouin scattering," *IEEE Photon. Technol. Lett.*, vol. 24, no. 14. pp. 1182–1184, Jul. 2012.

[12] D. Marpaung *et al.*, "Low-power, chip-based stimulated Brillouin scattering microwave photonic filter with ultrahigh selectivity," *Optica*, vol. 2, no. 2, pp. 76–83, Jan. 2015.

[13] H. Y. Jiang *et al.*, "Microwave photonic comb filter with ultra-fast tenability," *IEEE Photon. J.*, vol. 40, no. 21, pp. 4895–4898, 2015.

[14] H. Wang *et al.*, "Widely tunable single-bandpass microwave photonic filter based on polarization processing of a nonsliced broadband optical source," *Opt. Lett.*, vol. 38, no. 22, pp. 4857–4860, Nov. 2013.

[15] D. Marcuse, "Pulse distortion in single mode fibers," *Appl. Opt.*, vol. 19, no. 10, pp. 1653–1660, May 1980.

[16] S. L. Pan and Y. M. Zhang, "A tunable and wideband microwave photonic phase shifter based on a single sideband polarization modulator and a polarizer," *Opt. Lett.*, vol. 37, no. 21, pp. 4483–4485, Nov. 2012.

[17] W. Li, W. T. Wang, and N. H. Zhu, "Broadband microwave photonic splitter with arbitrary amplitude ratio and phase shift," *IEEE Photon. J.*, vol. 6, no. 6, Dec. 2014, Art. ID 5501507.